Numerical Heat Transfer, Part A, 45: 699–717, 2004

ISSN: 1040-7782 print/1521-0634 online
DOI: 10.1080/10407780490424307

Taylor & Francis
Taylor & Francis Group

NUMERICAL SOLUTIONS OF FLOWS IN ROCKET ENGINES WITH REGENERATIVE COOLING

Carlos Henrique Marchi
Department of Mechanical Engineering, Federal University of Paraná, Curitiba, PR, Brazil

Fernando Laroca
Federal University of Paraná, Curitiba, PR, Brazil

António Fábio Carvalho da Silva
Department of Mechanical Engineering, Federal University of Santa Catarina, Florianópolis, SC, Brazil

José Nivaldo Hinckel
Instituto Nacional de Pesquisas Espaciais, São José dos Campos, SP, Brazil

A one-dimensional mathematical model is presented for flows in a rocket engine that has a regenerative cooling system. The problem involves the flow of a gas in a converging-diverging nozzle, the flow of a coolant in channels distributed around the engine, and the heat conduction through a wall between the gas and the coolant. The numerical model adopted is based on the finite-volume method with a second-order scheme. It was noted that it is important to use variable properties in order to predict the maximum wall temperature in the rocket engine and the drop in pressure of the coolant as it moves along the channels, whereas the thrust of the engine can be calculated with constant properties.

INTRODUCTION

Many types of rockets having large dimensions use engines fueled by a liquid propellant and have a regenerative cooling system (Figure 1). For projects involving these engines, the key parameters of interest in this present work are the thrust (F) produced by the engine, the maximum temperature (T_{MAX}) reached in the wall, and the drop in pressure (Δp) of the coolant during its flow along the channels (Figure 2).

Received 3 April 2003; accepted 22 November 2003.

The first two authors would like to thank the Brazilian sponsors who supported this work: Federal University of Paraná (UFPR), Programa de Pós-Graduação em Engenharia Mecânica (POSMEC) of the Federal University of Santa Catarina, Coordenação de Aperfeiçoamento de Pessoal de Nível Superior (CAPES), and National Council for Scientific and Technological Development (CNPq).

Address correspondence to Carlos H. Marchi, Department of Mechanical Engineering, Federal University of Paraná, P.O. Box 19011, Curitiba, PR 81531-980, Brazil. E-mail: marchi@demec.ufpr.br

NOMENCLATURE

A	cross-sectional area	T	temperature
c_p	specific heat at constant pressure	u	velocity
D	diameter	x	length of flow along the center of the nozzle
F	thrust engine	Δp	drop in pressure of the coolant
h	convective heat transfer coefficient	ρ	density
$\dot{M}$	mass flow rate	**Subscripts**	
p	pressure	c	coolant
q	heat transfer rate	g	gas
q''	heat flux	MAX	maximum
R	gas constant	w	wall
s	length of the flow along the center of a channel	wc	coolant side wall
		wh	gas side wall

Determining the engine's thrust is of utmost importance in order to fulfill a rocket's mission: the payload mass, e.g., a satellite, and its orbit. Determining the distribution of temperatures along the wall and its maximum value is essential for one to predict an engine's lifetime and structural failure. Finally, determining the drop in pressure of the coolant along the channels is important in order to define the dimensions of its pumping system.

Many different phenomena are involved in the operations of rocket engines fueled by a liquid propellant [1–4]. Speaking in general terms, the fuel and the oxidizing agent, in a liquid state, are injected with a specific mass flow rate into the combustion chamber (Figure 1). After that, the propellant and oxidizing agent

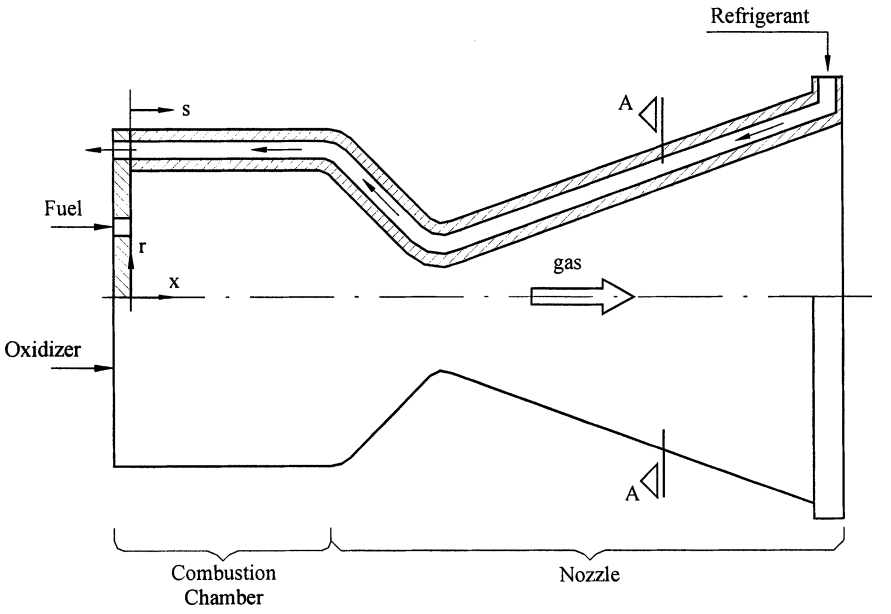

Figure 1. A liquid-propellant rocket engine with a regenerative cooling system.

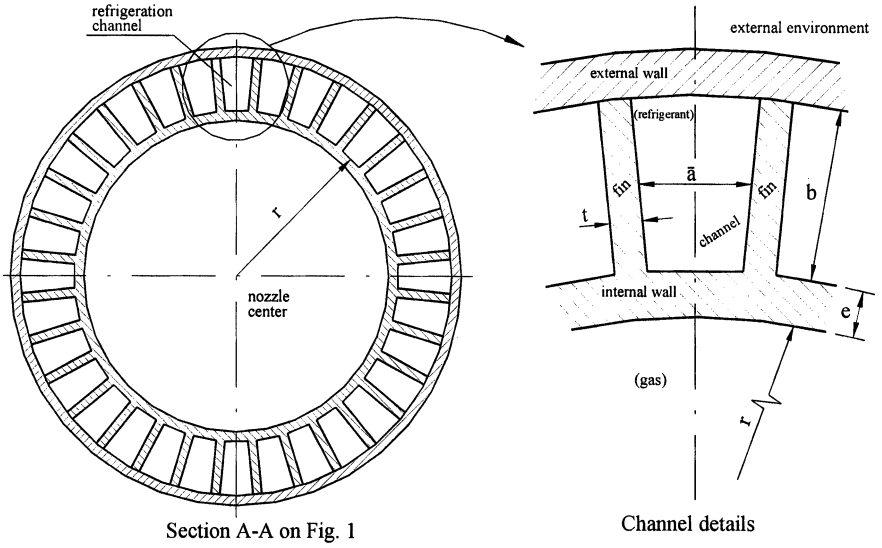

Figure 2. Geometric parameters for the cooling channels.

are atomized, mixed, and undergo chemical reactions, reaching high levels of pressure and temperature, and producing gases that flow through a converging-diverging nozzle. Due to the high thermal load imposed on the internal wall of the engine (Figure 2), this wall must be actively cooled for its temperature to be maintained within acceptable limits. Generally speaking, the fuel itself is used as a coolant before being injected into the combustion chamber. The gases start off at subsonic speeds while they are in the chamber, reach transonic speeds in the region where the nozzle narrows (the neck), and attain supersonic speeds as they leave the nozzle.

In the Vulcain engine [5, 6] of the Ariane 5 rocket, for example, the oxidizing agent is liquid oxygen and the fuel/coolant is liquid hydrogen. The internal wall of the engine as well as the fins of the channels (Figure 2) are made of copper, and the external wall is made of nickel. The thrust, at sea level, is 1,007 kN, the maximum temperature of the wall reaches 750 K, and the drop in pressure of the coolant is 23 bar. The values for the pressure and temperature of the gases in the combustion chamber are approximately 100 bar and 3,500 K, and the flow of mass of the gases is 232.3 kg/s. The heat flux in the internal wall next to the gases reaches 60 MW/m^2 in the region of the neck of the nozzle. The height (b) and the width (a) of the channels (Figure 2) range from 9.5 to 12 mm and from 1.3 to 2.6 mm, respectively, with the mass flow rate of the coolant being 33.7 kg/s when adding up all of the 360 channels of this engine. The diameter of the chamber and of the neck of the nozzle are 0.415 and 0.262 m, and the total length of the engine with refrigeration running countercurrent is 0.75 m.

In the real problem posed, the processes for determining F, T_{MAX}, and Δp may be divided up into three coupled subproblems, defined as follows [4, 5]:

1. The turbulent reactive flow of a mixture of gases in a rocket engine (Figure 1) made up of a combustion chamber and a converging-diverging nozzle

2. The heat conduction through the wall of the rocket engine between the gases it holds inside and the liquid coolant (Figure 2)
3. The turbulent flow of the liquid coolant in the channels located around the rocket engine (Figure 2)

One of the conclusions reached in the work carried out by Habiballah et al. [4] is that more progress is required in validation through experimentation, in modeling the phenomena involved in determining F, T_{MAX}, and Δp, and in developing numerical methods that will take less time to compute. For example, in the case of the three-dimensional numerical solution for the flow of liquid hydrogen in the channels of the Vulcain engine, it takes tens of hours to compute on an IBM 350 workstation with a relatively coarse grid [5]. Due to the amount of time required to carry out this computation, even nowadays, projects involving rocket engines have essentially been built using one-dimensional models and empirical correction factors [5].

Therefore, the main objective of the present study is to put forward a one-dimensional mathematical model, and the numerical model needed to solve it, in order to determine F, T_{MAX}, and Δp. These models are applied to a hypothetical problem. Numerical results are shown, along with their estimated numerical errors. How these results are affected is also compared when properties maintaining constant values or properties holding variables are adopted for the gas, the coolant, and the wall.

Great difficulties are faced when trying to find in relevant literature enough data to enable comparisons to be made of experimental or numerical results for the problem considered in this present study. Hence, due care has been taken in this work to define clearly all the data deemed necessary to enable future comparisons by other authors, so that they may analyze the mathematical and numerical models adopted in this study. Furthermore, estimates have been provided regarding the numerical errors in the results presented, to further facilitate future comparisons.

The following will be presented in subsequent sections: the mathematical model used, which takes into account, among other factors, the effects of area and variable properties; the shearing stress produced by viscous forces, and the heat transfer to the wall by convection and radiation; the numerical model, which uses the finite-volume method to solve the problems related not only to the flow of gases but also to the flow of the liquid coolant; the definition of the problem; the numerical results and the discussion of these results; and the conclusion of the study.

MATHEMATICAL MODEL

The mathematical model of the problem is divided up into three submodels. The first submodel is related to the flow of the mixture of gases inside the chamber-nozzle. The second one is for the flow of coolant within the channels. The third is related to the heat conduction through the wall of the rocket engine. The mathematical models put to use in these latter two subproblems are quite similar to those used by Rubin and Hinckel [7] and Rubin [8], and the mathematical model used for the flow of gases is basically the one adopted by Laroca et al. [9].

Gas Flow

The main simplifications made regarding the real problem are: the flow is one-dimensional and nonreactive; and the fluid which flows is a gas holding a constant composition, being of one single species and thermally perfect. The flow of this gas in the interior of the rocket engine is modeled through the mass conservation equation, the momentum equation, and the energy equation, as well as by the perfect gas law. These equations are represented respectively as follows:

$$\frac{d}{dx}(\rho_g u_g A) = 0 \tag{1}$$

$$\frac{d}{dx}(\rho_g u_g^2 A) = -A\frac{dp_g}{dx} + F' \tag{2}$$

$$c_{pg}\frac{d}{dx}(\rho_g u_g A T_g) = u_g A\frac{dp_g}{dx} + q' \tag{3}$$

$$p_g = \rho_g R T_g \tag{4}$$

In the momentum equation, Eq. (2), the mathematical model takes into account the effects of advection, pressure, and friction (the shearing stress produced by viscous forces). On the other hand, in the energy equation, Eq. (3), the effects considered are those related to advection, compressibility, kinetic heating due to friction, and the loss of heat to the wall through convection and radiation.

In Eqs. (1)–(4), ρ_g, u_g, p_g, and T_g are the four dependent variables that represent density, velocity, pressure, and temperature of the gas; x is the independent variable and it represents the rocket engine's coordinated direction along the longitudinal axis (Figure 1); A is the cross-sectional area to the x axis along which the gas flow occurs; c_{pg} and R represent the specific heat at constant pressure and a gas constant; and F' and q' model the effects of the shearing stress produced by viscous forces and of the gain or loss of heat, whose values are given by

$$F' = -\frac{\pi}{8} f_g \rho_g u_g |u_g| D \tag{5}$$

$$q' = |u_g F'| + A'_{wh}(q''_h + q''_r) \tag{6}$$

where f_g and D represent the friction factor defined by Darcy and the diameter of the circular section that lies transversal to the x axis along which the gas flows; A'_{wh} is the area of the internal wall (A_{wh}) by the unit of length along x (Figure 2), which is in contact with the gas; q''_h and q''_r represent the heat fluxes by convection and radiation to the wall which, according to Huzel and Huang [2] and Bejan [10], are modeled as follows:

$$q''_h = h_g(T_{wh} - T_{aw}) \tag{7}$$

$$q''_r = \bar{\varepsilon}\sigma(T_{wh}^4 - T_g^4) \tag{8}$$

where h_g, T_{wh}, and σ represent, respectively, the convective heat transfer coefficient between the gas and the wall, the temperature of the wall next to the gas, and the Stefan-Boltzmann constant (5.67051×10^{-8} W/m^{2}K^4); T_{aw} and $\bar{\varepsilon}$ represent the adiabatic wall temperature [2] and the emissivity [10] between the gas and the wall, which are calculated according to

$$T_{aw} = T_g \left[1 + g \frac{(\gamma - 1)}{2} M^2 \right] \tag{9}$$

$$\bar{\varepsilon} = \left(\frac{1}{\varepsilon_w} + \frac{1}{\varepsilon_g} - 1 \right)^{-1} \tag{10}$$

where g and γ represent the recovery factor and the specific heat ratio; ε_w and ε_g represent the emissivity of the wall and of the gas; and M is the Mach number of the flow, given by

$$M = \frac{u_g}{\sqrt{\gamma R T_g}} \tag{11}$$

It is acknowledged that the model used to consider the effect of thermal radiation according to Eqs. (8) and (10) is highly simplified. Nonetheless, it represents a way in which to study this effect of the real problem, where thermal radiation is of great importance due to the high temperatures involved [1].

The mathematical model shown above, in Eqs. (1)–(11), enables the problems of flow to be solved with A, c_{pg}, f_g, h_g, g, $\bar{\varepsilon}$, and T_{wh} variables with x, in addition to the unknowns u_g, p_g, T_g, and ρ_g.

Coolant Flow

The main simplification used with respect to the real problem was to consider the flow to be one-dimensional. The coolant flow inside the channels is modeled through the mass conservation equation, the momentum equation, the energy equation, and also by a polynomial constitutive equation, which are provided respectively by

$$\frac{d}{ds}(\rho_c u_c A) = 0 \tag{12}$$

$$\frac{d}{ds}(\rho_c u_c^2 A) = -A \frac{dp_c}{ds} + F' \tag{13}$$

$$c_{pc} \frac{d}{ds}(\rho_c u_c A T_c) = \beta T_c u_c A \frac{dp_c}{ds} + q' \tag{14}$$

$$\rho_c = \rho_1 + \rho_2 T_c + \rho_3 T_c^2 \tag{15}$$

In the momentum equation, Eq. (13), the mathematical model takes into consideration the effects of advection, pressure, and friction (the shearing stress

produced by viscous forces). On the other hand, in the energy equation, Eq. (14), the effects considered are those related to advection, expansion, and the gain of heat in the wall due to the kinetic heating caused by friction.

In Eqs. (12)–(15), ρ_c, u_c, p_c, and T_c, are the four dependent variables that represent density, velocity, pressure, and temperature of the coolant; s is the independent variable that represents the length of the flow along the center of a channel (Figure 1), this being measured from the point at which the coolant leaves the channels; A is the cross-sectional area to the s direction along which the coolant flow occurs; c_{pc} and β represent the specific heat at constant pressure and the volumetric thermal expansion coefficient; ρ_1, ρ_2, and ρ_3 are constants linked to each type of coolant, assuming that its density may be represented by a squared polynomial; F' is given by Eq. (5), only considering D as the hydraulic diameter of the channel; and q' is given by

$$q' = |u_c F'| + A'_{wc} q''_c \tag{16}$$

where A'_{wc} represents A_{wc} by the unit of length along s; A_{wc} is the area of the heat transfer between the coolant and the walls which constrain it, defined in Eq. (22). The heat flux q''_c is provided by [10]

$$q''_c = h_c(T_{wc} - T_c) \tag{17}$$

where h_c and T_{wc} represent the convective heat transfer coefficient between the coolant and the wall, and the temperature of the internal wall next to the coolant.

The mathematical model displayed above, in Eqs. (12)–(17), enables the problems of flow to be solved with A, c_{pc}, f_c, h_c, β, and T_{wh} variables with s, in addition to the unknowns u_c, p_c, T_c, and ρ_c.

Heat Conduction Through the Wall

The gas heat fluxes by convection and radiation affect the wall and are transmitted by conduction through the wall until they are transported by convection to the coolant. This process is modeled by

$$q = (q''_h + q''_r)A_{wh} = q''_w A_{wh} = q''_c A_{wc} \tag{18}$$

where q is the heat transfer rate through the wall; A_{wh} is the area of the rocket engine's internal wall (Figure 2) in contact with the gas; A_{wc} represents the effective area of heat transfer between the wall and the coolant; and q''_w represents the heat flux through the wall obtained by

$$q''_w = \frac{\bar{k}_w}{e}(T_{wh} - T_{wc}) \tag{19}$$

with

$$\bar{k}_w = k_1 + \frac{k_2}{2}(T_{wc} + T_{wh}) + \frac{k_3}{3}\frac{(T^3_{wh} - T^3_{wc})}{(T_{wh} - T_{wc})} \tag{20}$$

where

$$k_w = k_1 + k_2 T_w + k_3 T_w^2 \tag{21}$$

In Eq. (21), T_w is the wall temperature, which varies along its thickness e; and k_1, k_2, and k_3 are constants that define the material of which the wall is made, assuming that its thermal conductivity may be described by a squared polynomial. Equations (19) and (20) represent the analytical solution of the one-dimensional heat conduction in a radial direction, for k_w given by Eq. (21) and without the effect of the radius, that is, the heat conduction is considered to occur in a one-dimensional manner along a plane wall.

The effective area of heat transfer between the wall and the coolant, A_{wc}, is given by

$$A_{wc} = A_b + A_a \eta \tag{22}$$

where A_b is the area at the base of the channel (Figure 2) that is in contact with the coolant; A_a is the area of the fins in contact with the coolant; and η represents the fin efficiency. The area of the rocket engine's external wall (Figure 2) in contact with the coolant is considered adiabatic, and has thus not been taken into consideration in Eq. (22).

The coupling of the three subproblems, whose mathematical models were presented above, will be explained in the following section.

NUMERICAL MODEL

The numerical model used to solve the gas and coolant flows is based on the finite-volume method [11]. The solution domains through which the gas and coolant flows occur (Figure 1) are divided up into n control volumes in the x and s directions. These control volumes may have constant or variable length along each of the two solution domains.

The conservation equations of the mathematical model, Eqs. (1)–(3) and (12)–(14), are integrated based on each control volume basically following the procedure defined by Marchi and Maliska [12]. An alteration is made in the present work in that linear interpolation (second-order scheme) is used with deferred correction in the manner presented in the work carried out by Lilek et al. [13]. This integrating process results in a system of algebraic equations for each conservation equation, which is solved using the tri-diagonal matrix method (TDMA) [11, 14]. The mass conservation equation, Eq. (1) or (12), is adopted to obtain the pressure p. The momentum equation, Eq. (2) or (13), is used to obtain the velocity u. The energy equation, Eq. (3) or (14), is used to determine temperature T. The density ρ is obtained through Eq. (4) or Eq. (15).

The iteration process used to solve the mathematical model provided by Eqs. (1)–(4) or (12)–(15) goes, along general lines, as follows:

1. The data are read.
2. Initial estimates for the solutions for u, p, T, and ρ are made.

3. The thermophysical properties and other parameters (c_p, k, f, h, etc.) are calculated.
4. The coefficients of the system of algebraic equations are calculated for the momentum equation and the solution to u is obtained.
5. The coefficients of the system of algebraic equations are calculated for the energy equation and the solution to T is obtained.
6. The value of ρ is calculated.
7. The coefficients of the system of algebraic equations are calculated for the mass conservation equation and the solution to p is obtained.
8. One must return to step 3 until the desired number of iterations is reached.

Boundary Conditions for the Gas Flow

The boundary conditions applied to solve the mathematical model made up of Eqs. (1)–(4) are defined as follows at the inlet of the combustion chamber: T_g and p_g are fixed and are designated by the symbols T_o and p_o; u_g is extrapolated linearly starting from the two control volumes adjacent to the boundary; and ρ_g is obtained from Eq. (4) with T_o and p_o. At the outlet of the nozzle, the boundary conditions are: p_g, T_g, and u_g are extrapolated linearly starting from the two control volumes adjacent to the boundary; and ρ_g is obtained from Eq. (4) with extrapolated p_g and T_g.

Boundary Conditions for the Coolant Flow

The boundary conditions applied to solve the mathematical model made up of Eqs. (12)–(15) are defined as follows at the inlet of the channels: T_c and u_c are fixed and are designated by the symbols T_{in} and u_{in}; p_c is extrapolated linearly starting from the two control volumes adjacent to the boundary; and ρ_c is obtained from Eq. (15) and is designated as ρ_{in}. At the outlet of the channels, the boundary conditions are: T_c and u_c are extrapolated linearly starting from the two control volumes adjacent to the boundary; p_c is defined as being equal to zero; and ρ_c is obtained from Eq. (15).

Coupling of the Gas and Coolant Flows with Heat Conduction Through the Wall

The algorithm adopted to solve the mathematical model, which involves Eqs. (1)–(22), using the numerical model described above, is, along general lines, as follows.

1. The temperature distribution of the wall next to the gas of the rocket engine (Figure 2) is estimated. It is designated as T_{wh}.
2. The gas flow is solved with Eqs. (1)–(4) obtaining the values of u_g, p_g, T_g, ρ_g, and q_g, where

$$q_g = (q''_h + q''_r)A_{wh} \tag{23}$$

with the values for q''_h and q''_r provided by Eqs. (7) and (8).

3. The coolant flow is solved with Eqs. (12)–(15) obtaining the values of u_c, p_c, T_c and ρ_c.
4. The heat transfer rate between the gas and the coolant (q_T) is calculated through the equation

$$q_T = \frac{(T_{aw} - T_c)}{R_T} \tag{24}$$

where R_T represents total thermal resistance, whose value is determined by

$$R_T = R_g + R_w + R_c \tag{25}$$

with

$$R_g = \frac{(T_{aw} - T_{wh})}{[h_g(T_{aw} - T_{wh}) + \bar{\varepsilon}\sigma(T_g^4 - T_{wh}^4)]A_{wh}} \tag{26}$$

$$R_w = \frac{e}{\bar{k}_w A_{wh}} \tag{27}$$

$$R_c = \frac{1}{h_c A_{wc}} \tag{28}$$

5. T_{wh} and T_{wc} are found through the equations

$$T_{wh} = T_{aw} - q_T R_g \tag{29}$$

$$T_{wc} = T_{wh} - q_T R_w \tag{30}$$

and then, one must go back to step 3 until the variation in Δp can meet some criterion of convergence or until the number of iterations specified is reached. Equations (29) and (30) are obtained from Eq. (18) and their respective gradients of temperature and thermal resistance.

6. An error is calculated between the solutions for q_g and q_T, and given as a percentage. This error should be equal to zero when the iteration process has become fully converged. This error is represented by the symbol Δq, and its mathematical expression is as follows:

$$\Delta q = 100 \frac{\left\{ \sum_{i=1}^{n} \left[(q_g)_i - (q_T)_i \right] \right\}}{\sum_{i=1}^{n} (q_T)_i} \tag{31}$$

with the values for q_g and q_T being given by the Eqs. (23) and (24); i represents each control volume and n represents the total number of control volumes used to

determine each of the two solution domains, one being that of the gas flow and the other that of the coolant flow.

7. At this point, one must return to step 2 above, until Δq reaches any level of tolerance previously defined or until the desired number of iterations is reached.

Step 2. forms the iteration cycle for obtaining the solution for the gas flow, and steps 3–5 form the cycle for the coolant flow together with the heat conduction through the wall. Finally, steps 1–7 represent the overall iteration cycle of the problem, which incorporates both the solution for the gas and coolant flows as well as for the heat conduction through the wall.

DEFINING THE PROBLEM

The specific problem that is being dwelt upon in this study is defined below. It is a totally hypothetical problem which nonetheless involves real typical data for liquid-propellant rocket engines of large dimensions with a regenerative cooling system.

The geometric parameters of the rocket engine are shown in Figure 3. It is made up of a combustion chamber, which is a cylindrical section having a radius r_{in} and length L_c, and of a nozzle having length L_n, which is defined by a cosine curve. The radius r of the nozzle for $x \geqslant L_c$ is given by the equation

$$r = r_g + \frac{(r_{in} - r_g)}{2}\left\{1 + \cos\left[2\pi\frac{(x - L_c)}{L_n}\right]\right\} \tag{32}$$

where r_g is the radius at the neck of the nozzle. The values used are $r_{\text{in}} = 0.3$ m; $r_g = 0.1$ m; $L_c = 0.1$ m; and $L_n = 0.4$ m. Therefore, the rocket engine has a total length of $L_T = 0.5$ m, the contraction and expansion ratios in the convergent and divergent areas of the nozzle are equal to 9; and the radius of curvature of the neck is

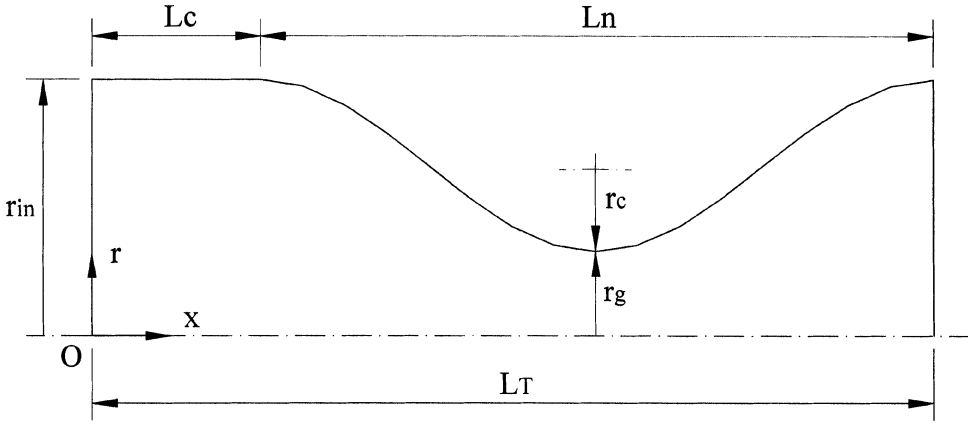

Figure 3. Geometric parameters for the rocket engine.

$r_c = 4.053 \times 10^{-2}$ m. For engines having large dimensions, the contraction ratio of areas is generally below 2 and the expansion ratio is over 50.

The number (m) of channels used placed around the rocket engine to flow the coolant is $m = 200$. Each one of these channels is defined by the parameters e, b, and t, shown in Figure 2. These letters mean: e, the thickness of the internal wall of the rocket engine; b, the height of each channel through which coolant is flowed; and t, the thickness of the wall that divides each channel, that is, the thickness of the fins of the channel. The values used are: $e = 2$ mm; $b = 5$ mm; and $t = 1.5$ mm. The parameter $\bar{a}$, shown in Figure 2, represents the average width of each channel; its value is a function of the previous parameters:

$$\bar{a} = \frac{\pi}{mb}\left[(r + e + b)^2 - (r + e)^2\right] - t \tag{33}$$

when $m > 1$. Even when e, b, and t remain constant, $\bar{a}$ is not constant, due to the variations in the radius r of the nozzle. For the data above, the ratio between the height and the average width of the channel results in roughly $b/\bar{a} = 0.62 - 2.8$.

The channels cover the whole length of the rocket engine (L_T), accompanying the variable radius of the nozzle. Copper for commercial uses was considered as the material used in the walls of the rocket engine. The gas flow moves along the x axis in a positive direction, whereas the coolant flow moves in a negative direction.

Given the data above, some key geometric parameters, to four significant figures are: $A_{wh} = 9.242 \times 10^{-1}$ m^2, $A_b = 7.272 \times 10^{-1}$ m^2, $A_a = 1.371$ m^2, and the ratio between the total length of flow covered by the coolant in the center of a channel and L_T is 1.371.

The liquid which flows in the combustion chamber and the nozzle is H_2O. The conditions at the inlet of the combustion chamber are: pressure, $p_o = 20$ bar; temperature, $T_o = 3,424.2$ K; specific heat ratio, $\gamma_o = 1.16695$; and the gas constant, $R = 461.525$ J/kg K.

The coolant which flows in the channels is water, having a temperature of $T_{\text{in}} = 300$ K at the inlet of the channels, and the total mass flow rate in the 200 channels is 200 kg/s. This situation applies to an engine that is to be tested on the ground with an independent cooling system. In real engines an additional restriction exists, that is, the availability of liquid coolant is limited according to the amount of fuel consumed by the engine and used as liquid coolant. This limitation has a great impact on the engine's scalability because the ratio of the cooling area to the volume of the chamber can vary greatly according to the size of the engine.

The aim of the numerical simulations is to obtain the solution to the mathematical model described for the following parameters of interest:

1. *The nozzle discharge coefficient (C_d)*: the ratio between the numerical ($\dot{M}_n$) and analytical ($\dot{M}_a$) solutions regarding the mass flow rate flowing in the nozzle, that is,

$$C_d = \frac{\dot{M}_n}{\dot{M}_a} \tag{34}$$

2. *The nondimensional momentum thrust (F^*):* the ratio between the numerical (F_n) and analytical (F_a) solutions regarding the momentum thrust produced by the nozzle, or rather,

$$F^* = \frac{F_n}{F_a} \tag{35}$$

where

$$F = \dot{M} u_{\text{ex}} \tag{36}$$

and u_{ex} represents the velocity at which the gas comes out of the nozzle.

3. *The maximum wall temperature* (T_{MAX}), obtained from the distribution of temperature T_{wh}.
4. *The drop in pressure of the coolant* (Δp) from when it enters to when it leaves the channels.
5. *The temperature of the coolant when it leaves the channels* (T_{ex}).

The analytical solution [15] of the one-dimensional isentropic flow in the nozzle for the rocket engine defined above results in $\dot{M}_a = 3.208932 \times 10^1$ kg/s, $F_a = 1.009365 \times 10^5$ N, $u_{\text{ex}} = 3.145486 \times 10^3$ m/s, $c^* = 1.958030 \times 10^3$ m/s, $C_F = 1.606454$, $I_s = 3.207503 \times 10^2$ s, $M_g = 1$, and $M_{\text{ex}} = 3.117115$. Here, c^*, C_F, and I_s represent, respectively, the characteristic velocity, the thrust coefficient, and the thrust-chamber specific impulse, as defined by Sutton [1], and M_g and M_{ex} represent the Mach number at the neck and at the exit of the nozzle, respectively.

NUMERICAL RESULTS

Results are shown as follows for the two types of numerical simulations that were carried out: (1) using constant properties for the gas, the coolant, and the wall; and (2) using variable properties.

Constant Properties

In addition to the data presented in the previous section, the numerical solutions for constant properties were obtained using the following additional data:

1. For the gas flow: $f_g = 2.40 \times 10^{-3}$; $h_g = 1.60 \times 10^3$ W/m^2 K; $g = 1$; $\bar{\varepsilon} = 0.25$; $c_{pg} = \gamma_o R/(\gamma_o - 1)$.
2. For the coolant flow: $f_c = 3.90 \times 10^{-3}$; $h_c = 3.10 \times 10^4$ W/m^2 K; $\eta = 0.50$; $\beta = 0$; $\rho_1 = 996.10$ kg/m^3; $\rho_2 = \rho_3 = 0$; $c_{pc} = 4.180 \times 10^3$ J/kg K.
3. For the wall: $k_1 = 376.50$ W/m K; $k_2 = k_3 = 0$.

The values above were obtained from the results of the simulations using variable properties, which are reported below. These values are the conditions at the

inlet of the combustion chamber for the gas flow and the conditions at the inlet of the channels for the coolant flow. These values are considered the natural choice for simulations with constant properties, except with regard to the efficiency of the fins, for which an average value was assumed between the minimum (0) and maximum (1) values possible. Another exception is that of $\bar{\varepsilon}$, for which a value was simply fixed.

Aiming to take into consideration the two-dimensional effect of the nozzle on the one-dimensional gas flow, the value established for the pressure at the inlet of the combustion chamber, $p_o = 20$ bar, was altered to the product of $p_o\psi$. The correction factor ψ is the theoretical discharge coefficient, according to Kliegel and Levine [16], calculated based on γ_0 and the ratio between r_c and r_g. For the nozzle under analysis, shown in Figure 3, the result was $\psi = 0.9750$. Hence, in the simulations, $p_o = 19.50$ bar was used, but the value of 20 bar was maintained to calculate the analytical solution already presented.

The results obtained for the five parameters of interest (C_d, F^*, T_{MAX}, Δp, and T_{ex}) and their respective estimated numerical errors are presented in Table 1, for each solution domain defined by $n = 1,280$ control volumes. These errors refer only to the discretization errors [11] that exist in the numerical solution of the mathematical model of the problem. These errors do not consider so-called modeling errors, that is, errors related to the mathematical model taken up to depict the real problem.

Variable Properties

To obtain the numerical solutions using variable properties, the data presented in the previous section were used, and the following additional data were included:

1. For the gas flow:
   f_g: Miller's equation [17] with the absolute rugosity of the wall equal to 5×10^{-6} m
   h_g: Bartz's equation [18]
   $g = \mathrm{Pr}^{1/3}$
   $\bar{\varepsilon} = 0.250$
   $\gamma = c_{pg}/(c_{pg} - R)$
   where the Prandtl number is $\mathrm{Pr} = c_{pg}\mu/k$, and μ and k represent, respectively, dynamic viscosity and thermal conductivity.

Table 1. Results for constant properties with 1,280 control volumes

Parameter	Numerical result and its estimated error
C_d	$0.980260 \pm 3 \times 10^{-6}$ (nondimensional)
F^*	$0.974764 \pm 5 \times 10^{-6}$ (nondimensional)
T_{MAX}	$497.148 \pm 6 \times 10^{-3}$ K
Δp	$7.61096 \pm 7 \times 10^{-5}$ bar
T_{ex}	$306.778 \pm 1 \times 10^{-3}$ K

$c_{pg}(T_g)$, $\mu;(T_g)$, and $k(T_g)$: equations by McBride et al. [19] for $H_2O_{(g)}$ are given by

$$c_p(T) = R(c_{p1} + c_{p2}T + c_{p3}T^2 + c_{p4}T^3 + c_{p5}T^4) \tag{37}$$

$$\mu(T) = 10^{-7}\exp(\mu_1 \ln T + \frac{\mu_2}{T} + \frac{\mu_3}{T^2} + \mu_4) \tag{38}$$

$$k(T) = 10^{-4}\exp\left(k_1 \ln T + \frac{k_2}{T} + \frac{k_3}{T^2} + k_4\right) \tag{39}$$

where c_{pi}, μ_i and k_i are constants.

2. For the coolant flow:
   f_c: Miller's equation [17] with the absolute rugosity of the wall equal to 5×10^{-6} m
   h_c: Gnielinski's equation [20]
   η: Bejan's equation [10] for rectangular fins with isolated tips
   $\beta = -(\rho_2 + 2\rho_3 T_c)/\rho_c$, according to the definition for β provided by Bejan [10] and ρ_c provided by Eq. (15)
   $\rho_c(T_c)$: Eq. (15) with $\rho_1 = 751.5644$ kg/m^3, $\rho_2 = 1.891228$ kg/m^3 K, and $\rho_3 = -3.5873915 \times 10^{-3}$ kg/m^3 K^2, for the polynomial as adjusted to the data listed [10] for $H_2O_{(l)}$
   $c_{pc}(T_c)$: equation by McBride et al. [19] for $H_2O_{(l)}$ provided by Eq. (37)
   $\mu(T_c)$ and $k(T_c)$: equations by Reid et al. [21] for $H_2O_{(l)}$; $k(T_c)$ is given by Eq. (21) and $\mu(T_c)$ by

$$\mu(T) = 10^{-3}\exp\left(\mu_1 + \frac{\mu_2}{T} + \mu_3 T + \mu_4 T^2\right) \tag{40}$$

3. For the wall: $k_w(T_w)$: Eq. (21) with $k_1 = 385.875$ W/m K, $k_2 = -2.600 \times 10^{-3}$ W/m K^2, and $k_3 = -5.006 \times 10^{-5}$ W/m K^3, according to Rubin [8] for the data listed by Sutton [1]

The same consideration made above regarding p_o for constant properties was also made here, that is, the value $p_o = 19.50$ bar was used. The results obtained for the five parameters of interest (C_d, F^*, T_{MAX}, Δp, and T_{ex}) and their respective estimated numerical errors are presented in Table 2. The estimates of the numerical (discretization) errors shown in Tables 1 and 2 were reached based on the GCI (Grid Convergence Index) estimator [22], which can be expressed as

$$\mathrm{GCI}(\phi_1) = 3\frac{|\phi_1 - \phi_2|}{(r^p - 1)} \tag{41}$$

Table 2. Numerical results and their estimated errors for variable properties

Parameter	80 control volumes	1,280 control volumes
C_d	0.985 $\pm 3 \times 10^{-3}$ (nondimensional)	0.984457 $\pm 4 \times 10^{-6}$ (nondimensional)
F*	0.975 $\pm 5 \times 10^{-3}$ (nondimensional)	0.973851 $\pm 6 \times 10^{-6}$ (nondimensional)
T_{MAX}	615.1 $\pm 3 \times 10^{-1}$ K	615.331 $\pm 2 \times 10^{-3}$ K
Δp	8.4 $\pm 3 \times 10^{-1}$ bar	8.37897 $\pm 6 \times 10^{-5}$ bar
T_{ex}	311.2 $\pm 1 \times 10^{-1}$ K	311.200 $\pm 1 \times 10^{-3}$ K

where ϕ is each parameter of interest; ϕ_1 and ϕ_2 indicate two numerical solutions obtained on two different grids, fine (h_1) and coarse (h_2); r is the grid refinement ratio ($r = h_2/h_1$); h is the grid spacing or distance between two successive grid points; and p is the order of the numerical model truncation error. In this work, $p = 2$ because the numerical model adopted is a second-order scheme. We employed grids with 10, 20, 40, 80, 160, 320, 640, and 1,280 control volumes, that is, $r = 2$.

The temperature distribution of the wall next to the gas (T_{wh}), of the wall next to the coolant (T_{wc}), and of the coolant (T_c) are shown in Figure 4, along with the profile of the rocket engine. Tables 3 and 4 show the variation ranges seen along x of the several properties of the gas, the coolant, and the wall, where the x coordinate is indicated when it hits its minimum and maximum values. It must be recalled that the point where $x = 0$ represents the beginning point in the combustion chamber (Figure 3), the point at which the gas starts to be flowed, and that $x = 0.5$ indicates the total length of the engine, the coordinate at which point the coolant enters the channels. The coordinate for the neck of the nozzle is $x_g = 0.3$.

The iteration cycle used to solve the problems of the gas and coolant flows was carried out until round-off error was reached. In this case, the iteration and the round-off errors do not affect the first 12 significant figures in any of the variables of interest in any one of the simulations made. The number of iterations required to ensure this, for variable properties, fluctuates from 2,000 to 35,000 in the case of the gas flow, and from 1,000 to 3,000 in the case of the coolant flow, with the number of control volumes ranging from 10 to 1,280.

On the other hand, the iteration cycle upon coupling of the gas and the coolant flows with heat conduction through the wall requires only 10–20 iterations for it to

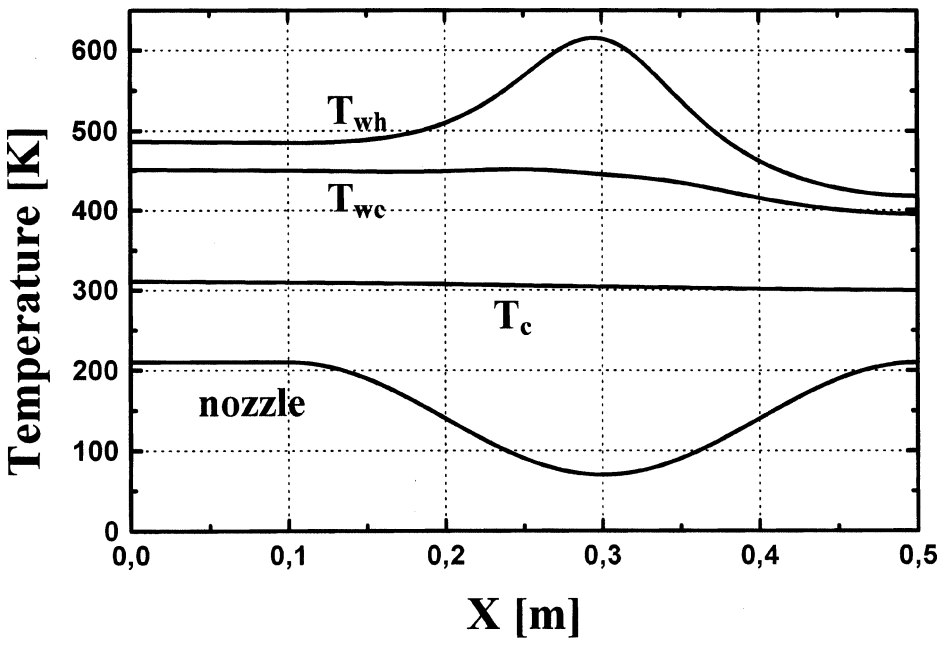

Figure 4. Wall and coolant temperatures for variable properties.

Table 3. Gas flow results for variable properties with 1,280 control volumes

Property	Minimum value (x)	Maximum value (x)
f_g (nondimensional)	2.104×10^{-3} (0.330)	2.396×10^{-3} (zero)
h_g (W/m^2 K)	1.376×10^{3} (0.500)	1.102×10^{4} (0.299)
c_{pg} (J/kg K)	2.751×10^{3} (0.500)	3.226×10^{3} (zero)
γ (nondimensional)	1.167 (zero)	1.202 (0.500)
μ (Pa s)	6.278×10^{-5} (0.500)	1.056×10^{-4} (zero)
k (W/m K)	2.067×10^{-1} (0.500)	4.719×10^{-1} (zero)
g (nondimensional)	8.969×10^{-1} (zero)	9.419×10^{-1} (0.500)
$\lvert q''_{wh} \rvert$ (W/m^2)	4.221×10^{6} (0.500)	3.146×10^{7} (0.297)
$\lvert q''_r/(q''_r + q''_h) \rvert$ (nondimensional)	3.025×10^{-2} (0.500)	2.942×10^{-1} (zero)

reach round-off error in the case of simulations using variable properties. However, five iterations alone are enough for the iteration error to be more than 1,000 times smaller than the errors mentioned in Table 2 that refer to discretization errors for 1,280 control volumes.

Using a Pentium IV PC of 1.6 GHz and Fortran 90 language in the implementation of the computational code, the time required to compute the results mentioned in Tables 1 and 2, with $n = 1,280$ control volumes, was 1.5 min and 18.3 min for constant and variable properties, respectively. When only $n = 80$ control volumes were used, the time required to compute the results for variable properties was reduced to 8 s. These results are shown in Table 2. In this case, it should be noted that the estimated numerical error for C_d, for example, is of the same order as the errors obtained through experimentation. In three similar nozzles, Back et al. [23] estimated the error in C_d obtained through experimentation to be in the range ± 0.005 to ± 0.008. Hence, for the nozzle chosen in the present study, each simulation of the problem, targeting the project of the nozzle and its cooling system, could be carried out using the value of $n = 80$ control volumes.

Comparing the results obtained for constant properties (Table 1) to those obtained for variable properties (Table 2), it can be seen that the differences in C_d and F^* are smaller than the estimated experimental errors [23]. Nonetheless, the difference in the result of Δp is considerable, and the difference in T_{MAX} is very large (118 K). According to relevant literature [3, 5], an error of 40–50 K in the temperature of the wall will lead to a forecast which is 50% shorter for an engine's

Table 4. Coolant flow results for variable properties with 1,280 control volumes

Property	Minimum value (x)	Maximum value (x)
f_c (nondimensional)	3.824×10^{-3} (zero)	4.480×10^{-3} (0.300)
h_c (W/m^2 K)	3.066×10^{4} (0.500)	1.619×10^{5} (0.299)
c_p (J/kg K)	4.168×10^{3} (zero)	4.179×10^{3} (0.500)
μ (Pa s)	6.932×10^{-4} (zero)	8.716×10^{-4} (0.500)
k (W/m K)	6.192×10^{-1} (0.500)	6.344×10^{-1} (zero)
η (nondimensional)	2.633×10^{-1} (0.299)	5.639×10^{-1} (0.500)
β (K^{-1})	2.623×10^{-4} (0.500)	3.441×10^{-4} (zero)
q''_c (W/m^2)	2.920×10^{6} (0.500)	2.278×10^{7} (0.297)
k_w (W/m K)	3.703×10^{2} (0.293)	3.765×10^{2} (0.500)

lifetime. Differences have been reported of 100–200 K between experimental results and one-dimensional numerical results for the wall temperature in the chamber and in the divergent area of the nozzle, respectively.

CONCLUSION

A one-dimensional mathematical model was put forth for the gas flow in a liquid-propellant rocket engine coupled with the heat conduction in its wall and for the coolant flow on this wall inside the channels.

The numerical model implemented to solve the mathematical model is quick and accurate from the project's point of view. It is able to produce results with an estimated numerical error equivalent to the errors found through experimentation when the value of 80 control volumes was used. In this case, the time required to compute the results was 8 s when using a Pentium IV PC with 1.6 GHz.

It was noted that it is important to use variable properties in order to predict the maximum wall temperature in the rocket engine and the drop in pressure of the coolant as it moves along the channels, whereas the thrust of the engine can be calculated with constant properties.

REFERENCES

1. G. P. Sutton, *Rocket Propulsion Elements*, 6th ed., Wiley, New York, 1992.
2. D. K. Huzel and D. H. Huang, *Modern Engineering for Design of Liquid-Propellant Rocket Engines*, AIAA Progress in Astronautics and Aeronautics, vol. 147, 1992.
3. C. A. Schley, G. Hagemann, and V. Golovitchev, Comparison of High Pressure H_2/O_2 Rocket Model Engine Reference Simulations, *Proc. 31st Joint Propulsion Conf. and Exhibit*, San Diego, CA, AIAA 95–2429, 1995.
4. M. Habiballah, L. Vingert, V. Duthoit, and P. Vuillermoz, Research as a Key in the Design Methodology of Liquid-Propellant Combustion Devices, *J. Propulsion Power*, vol. 14, pp. 782–788, 1998.
5. A. Fröhlich, M. Popp, G. Schmidt, and D. Thelemann, Heat Transfer Characteristics of H_2/O_2–Combustion Chambers, *Proc. 29th Joint Propulsion Conf.*, Monterey, CA, AIAA 93–1826, 1993.
6. F. LeBail and M. Popp, Numerical Analysis of High Aspect Ratio Cooling Passage Flow and Heat Transfer, *Proc. 29th Joint Propulsion Conf.*, Monterey, CA, AIAA 93–1829, 1993.
7. R. L. Rubin and J. N. Hinckel, Regenerative Cooling for Liquid Propellant Rocket Thrust Chambers, *Proc. 12th Brazilian Congress of Mechanical Engineering*, Brasília, DF, Brazil, 1993.
8. R. L. Rubin, Regenerative Cooling for Liquid Propellant Rocket Thrust Chambers (in Portuguese, Refrigeração Regenerativa para Câmaras de Empuxo de Motores Foguete a Propelentes Líquidos), M.Sc. dissertation, Instituto Nacional de Pesquisas Espaciais, São José dos Campos, SP, Brazil, 1994.
9. F. Laroca, C. H. Marchi, and A. F. C. Silva, Solutions of Quasi-unidimensional Flows of Compressible and Viscous Fluids in Nozzles with Heat Transfer (in Portuguese, Soluções de Escoamentos Quase-Unidimensionais de Fluidos Compressíveis e Viscosos em Tubeiras com Troca de Calor), *Proc. 7th Brazilian Congress on Engineering and Thermal Sciences*, Rio de Janeiro, RJ, Brazil, pp. 1031–1036, 1998.
10. A. Bejan, *Heat Transfer*, Wiley, New York, 1993.

11. J. H. Ferziger and M. Peric, Computational Methods for Fluid Dynamics, 2nd ed., Springer-Verlag, Berlin, 1999.
12. C. H. Marchi and C. R. Maliska, A Nonorthogonal Finite-Volume Method for the Solution of All Speed Flows Using Co-Located Variables, *Numer. Heat Transfer B*, vol. 26, pp. 293–311, 1994.
13. Z. Lilek, S. Muzaferija, and M. Peric, Efficiency and Accuracy Aspects of a Full-Multigrid Simple Algorithm for Three-Dimensional Flows, *Numer. Heat Transfer B*, vol. 31, pp. 23–42, 1997.
14. L. H. Thomas, *Elliptic Problems in Linear Difference Equations over a Network*, Watson Sci. Comput. Lab. Report, Columbia University, New York, 1949.
15. J. E. A. John, *Gas Dynamics*, 2nd ed., Allyn & Bacon, Boston, 1984.
16. J. R. Kliegel and J. N. Levine, Transonic Flow in Small Throat Radius of Curvature Nozzles, *AIAA*, J., vol. 7, pp. 1375–1378, 1969.
17. R. W. Miller, *Flow Measurement Engineering Handbook*, 2nd ed., McGraw Hill, New York, 1983.
18. D. R. Bartz, A Simple Equation for Rapid Estimation of Rocket Nozzle Convective Heat Transfer Coefficients, *Jet Propulsion*, vol. 37, pp. 49–51, 1957.
19. B. J. McBride, S. Gordon, and M. A. Reno, Coefficients for Calculating Thermodynamic and Transport Properties of Individual Species, *NASA Tech. Memo. 4513*, Cleveland, OH, USA, 1993.
20. V. Gnielinski, New Equations for Heat and Mass Transfer in Turbulent Pipe and Channel Flow, *Int. Chem. Eng.*, vol. 16, pp. 359–368, 1976.
21. R. C. Reid, J. M. Prausnitz, and B. E. Poling, *The Properties of Gases & Liquids*, 4th ed., McGraw-Hill, New York, 1987.
22. P. J. Roache, Perspective: A Method for Uniform Reporting of Grid Refinement Studies, *J. Fluids Eng.*, vol. 116, pp. 405–413, 1994.
23. L. H. Back, R. F. Cuffel, and P. F. Massier, Influence of Contraction Section Shape and Inlet Flow Direction on Supersonic Nozzle Flow and Performance, *J. Spacecraft Rockets*, vol. 9, pp. 420–427, 1972.